Petrology of the Indian eucrite Piplia Kalan

P.C. Buchanan[1], D.W. Mittlefehldt[2], R. Hutchison[3],

C. Koeberl[4], D.J. Lindstrom[1], and M.K. Pandit[5]

[1]Mail Code:SN2, NASA Johnson Space Center, Houston, Texas 77058, U.S.A.

[2]C23, Lockheed Martin ESS, 2400 NASA Rd 1, Houston, Texas 77058, U.S.A.

[3]Mineralogy Department, The Natural History Museum, Cromwell Road,

London SW7 5BD, Great Britain

[4]Institute of Geochemistry, University of Vienna, Althanstrasse 14, A-1090 Vienna, Austria

[5]Department of Geology, University of Rajasthan, Jaipur 302004, India

Abstract

Piplia Kalan is an equilibrated eucrite consisting of 60-80 vol.% lithic clasts in a subordinate brecciated matrix. Ophitic/subophitic lithic clasts fall into two groups: finer-grained lithology A and coarser-grained lithology B. Very fine-grained clasts (lithology C) also occur and originally were hypocrystalline in texture. The variety of materials represented in Piplia Kalan suggests cooling histories ranging from quenching or fast crystallization to slower crystallization. Despite textural differences, clasts and matrix have similar mineral and bulk compositions. Thus, Piplia Kalan is probably best classified as a genomict breccia that could represent fragments of a single lava flow or shallow intrusive body, including fine-grained or glassy outer margin and more slowly cooled coarser-grained interior. Piplia Kalan displays evidence of an early shock event, including brecciated matrix and areas of lithic clasts that contain fine-grained, equigranular pyroxene between deformed feldspar laths. The meteorite also displays evidence of at least one episode of thermal metamorphism: hypocrystalline materials are recrystallized to hornfelsic textures and the matrix has a nonporous texture similar to those of eucrites that were affected by post-brecciation heating. Veins of brown glass transect both lithic clasts and brecciated matrix and indicate a second, post-metamorphism shock event.

1. INTRODUCTION

The Piplia Kalan meteorite fell on 20 June, 1996 in western India. Vaya et al. (1996) and Shukla et al. (1997a) provided information on the fall and recovery, initial petrographic and compositional information, and classification. The meteorite is an eucrite, composed predominantly of basaltic lithic clasts in a subordinate, fine-grained, brecciated matrix. Bhandari et al. (1998) reported a Pu/Xe age of 4.56 Ga and a Sm/Nd age of 4.574±0.018 Ga (Kumar and Gopalan, pers. comm.). The same authors suggested that the meteorite was subjected to a late-stage metamorphic event as evidenced by a K-Ar age of 2.2 Ga. A great deal of interest has centered on the recent report by Srinivasan et al. (1999) of excess ^{26}Mg in plagioclase of Piplia Kalan. These data are important because they provide evidence that the decay of ^{26}Al to ^{26}Mg may have been responsible for melting of the eucrite parent body (Srinivasan et al., 1999). Our study provides additional information about the petrogenetic history of this meteorite.

2. SAMPLES AND ANALYTICAL METHODS

The meteorite specimen was collected by one of us (MKP) at the site of the fall. The fragment was of approximately 30 g and was broken from the interior of one of the stones with very fresh surfaces and no remnants of fusion crust. Processing and sampling of the various lithologies represented in the meteorite were accomplished at the University of the Witwatersrand by PCB and at NASA Johnson Space Center (JSC), Houston, Texas by DWM. Thin sections of various lithologies were made at the Council of Geosciences, Pretoria, South Africa and at the thin section lab of NASA-JSC. Four thin sections were made for this study, and two additional thin sections were loaned by the Natural History Museum, London, U.K.

Mineral compositions reported in this paper were determined with the Cameca SX-100 electron microprobe at NASA-JSC and the ARL electron microprobe at the Naturhistorisches Museum, Vienna, Austria. Counting times for elements were 20-30 sec. Operating conditions were 15 kV and 15 nA for plagioclase and glass and 15 kV and 30 nA for pyroxenes and oxides. Natural and synthetic mineral standards were used and the data were corrected for absorption, fluorescence, and atomic number effects. Bulk compositions were acquired at NASA-JSC using standard INAA procedures. The samples plus standards and controls were encapsulated in pure silica glass tubes, and then irradiated at the Research Reactor Facility of the University of Missouri for 12 hours at a flux of 5.5×10^{13} n/cm^2-s. Details of the JSC INAA lab analysis and data reduction procedures are described in Mittlefehldt and Lindstrom (1991) and Mittlefehldt et al. (1992).

3. DATA

Original descriptions of Piplia Kalan are contained in Vaya et al. (1996) and Shukla et al. (1997a). In this section, we provide supplemental data that are relevant to the petrologic interpretation of the meteorite.

Petrography. The meteorite is composed of 60-80 vol.% angular to rounded, basaltic lithic clasts (up to ~1 cm in diameter in our samples) in a subordinate, brecciated matrix. Vaya et al. (1996) and Shukla et al. (1997a) noted that ophitic/subophitic lithic clasts in Piplia Kalan can be subdivided into two groups: finer-grained lithology A (average grain size <<1 mm) and coarser-grained lithology B (average grain size ~1 mm). Vaya et al. (1996) estimated that lithology A has a mode (vol.%) of 65% pyroxene, 25% plagioclase, 6% opaques, and 4% xenolithic components. Feldspars in this lithology are subhedral to euhedral, lath-shaped to

blocky grains that are randomly oriented and form a network with anhedral pyroxenes and opaques filling the interstices. Pyroxenes are honey-coloured, twinned and contain exsolution lamellae up to 10μm in width in a low-Ca pyroxene host.

Vaya et al. (1996) estimated a mode (vol.%) for coarser-grained lithology B of 55% pyroxene, 40% plagioclase, and 5% opaques, including ilmenite, chromite, and iron sulfide. Minor amounts of a silica mineral also are present. Feldspars are lath-shaped to blocky; pyroxenes are twinned and composed of augite exsolution lamellae (up to 10 μm in width) in a low-Ca pyroxene host. In some clasts of lithology B, ophitic/subophitic textures are gradational with areas composed of randomly oriented, lath-shaped feldspars with interstitial aggregates of fine-grained (average grain size 5-10 μm), equigranular pyroxenes and opaques (Fig. 1). There is some evidence that these aggregates were originally single pyroxene grains. Exsolution lamellae can, in some cases, be traced from one granule to adjoining granules. Feldspars in these areas have twins that are kinked or offset by small faults that transect crystals.

Also contained within Piplia Kalan are very fine-grained basaltic clasts with equigranular textures that are texturally similar to terrestrial hornfels. For convenience, we designate these materials as lithology C. Vaya et al. (1996) and Shukla et al. (1997a) describe xenoliths that are similar to lithology C and are contained within clasts of lithology A. Lithology C (Fig. 2a) is predominantly composed of fine-grained (grain size ~20-30 μm) honey-coloured pyroxene, colourless plagioclase, and minor opaques, including ilmenite and chrome spinel. The groundmass of lithology C is recrystallized to a fine-grained aggregate of equant grains of pyroxene and plagioclase. Pyroxene and plagioclase also occur as laths in lithology C. The pyroxene laths commonly are 20-50 μm wide and 300-500 μm long and, in many cases, are

recrystallized to chains of equant crystals that are similar to those in the groundmass (Fig. 2b). The plagioclase laths commonly display scalloped edges that apparently result from recrystallization of adjoining pyroxenes to equant crystals. The texture suggests that this lithology was originally composed of laths of pyroxene and plagioclase in a groundmass that was probably glassy. The clast of lithology C analyzed in this study has, on one side, a gradational boundary with an adjacent clast of lithology A. This boundary is characterized by concentrations of opaque mineral grains. Where this clast is in contact with the brecciated matrix of the meteorite, the boundary is, in some areas, vague and recrystallized and, in other areas, is followed by a glassy vein as described below.

The brecciated matrix of Piplia Kalan is fine-grained (average grain size <<0.5 mm) with little porosity and is predominantly composed of fragments of pyroxene and plagioclase with minor ilmenite, iron sulfide, and a silica mineral. Pyroxene fragments range from rounded to angular, whereas plagioclase fragments are irregular and, in some cases, display scalloped edges (Fig. 3). Matrix material varies in grain size throughout the meteorite. In some areas adjacent to lithic clasts this matrix is distinctly finer-grained than in other areas. The thin dark boundaries described by Shukla et al. (1997b) around some lithic clasts, may represent these finer-grained areas.

Thin, slightly curved or jointed veins of brown glass (Fig. 4) with maximum thicknesses of ~20 μm are also present throughout Piplia Kalan. They cross both matrix and clasts and, in some cases run along clast/matrix boundaries. Boundaries between the veins and surrounding material vary from smooth to irregular and the glass contains rare mineral fragments. Back-scattered electron images indicate that the glass varies somewhat in composition; long wavy

areas of slightly different image brightness parallel vein boundaries. A representative bulk glass composition determined by averaging several electron microprobe analyses is listed in Table 1. This composition is enriched in feldspar relative to the bulk composition of Piplia Kalan.

Pyroxene and plagioclase grains in both the matrix and lithic clasts of Piplia Kalan display undulating extinction; feldspars also commonly display incipient mosaicism and deformed twins. The centers of many of these mineral grains contain abundant inclusions (Fig. 5; see also Shukla et al., 1997b) that commonly are arranged along preferred crystallographic planes of the host minerals, including twin and lamellae boundaries. Similar inclusions were described as 'clouding' by Harlow and Klimentidis (1980). Piplia Kalan is particularly distinctive compared to other eucrites because these inclusions are relatively large (up to 5-10 μm in size) and spaced farther apart, and thus there are relatively broad areas that are inclusion-free. These inclusion-free areas allowed Srinivasan et al. (1999) to analyze feldspar with relatively low Mg/Al.

Mineral Compositions. Despite the variations in textures, mineral compositions are similar for the matrix and all lithologies (Figs. 6a-d; Tables 2, 3, 4). Pyroxenes display little evidence of original zoning and are composed of augite exsolution lamellae in a low-Ca pyroxene host. Compositions are slightly more ferroan than those of the eucrite Juvinas but more magnesian than those of Nuevo Laredo. Plagioclase compositions are intermediate in anorthite content between those of Juvinas and Nuevo Laredo.

Bulk Compositions. Bulk compositions determined in this study of the matrix and lithologies A and B are listed in Table 5. CI-normalized rare earth element (REE) abundances are shown in Fig. 7. Bulk compositions of two samples each of lithologies A and B were also

reported by Shukla et al. (1997a). The matrix sample has the highest REE^{3+} contents at 12-13 x CI, and a depletion of Eu, with a normalized Eu/Sm of 0.84±0.04. The two ophitic/subophitic lithologies have slightly lower REE^{3+} abundances (11-12 x CI for lithology A, 10-11 x CI for lithology B), but have Eu contents essentially identical to that of the matrix. The Eu/Sm ratios are 0.91±0.05 for lithology A and 1.05±0.05 for lithology B. The abundances of other lithophile elements vary from 0.45-0.75 x CI for Na and K, to ~5 x CI for Sc, and to 7-8 x CI for Ca. The abundances of most of these elements are similar to those of the main group eucrite Juvinas, and somewhat higher than those of the main group eucrite Sioux County (Jérome, 1970; Basaltic Volcanism Study Project, 1981).

4. DISCUSSION

Classification. Mineral compositions and bulk compositions are similar throughout the various lithologies of Piplia Kalan and there is no evidence of remanent zoning of pyroxene or plagioclase. Hence, the meteorite is classified as an equilibrated eucrite based on the work of Reid and Barnard (1980) and is a type 5 or 6 in the metamorphic grade of Takeda and Graham (1991). Based on bulk compositions, Shukla et al. (1997a) suggested that Piplia Kalan is a noncumulate eucrite. Pyroxene compositions and bulk major element compositions of the meteorite are much more ferroan than those typical of cumulate eucrites (e.g., Serra de Magé; Harlow et al., 1979) and incompatible lithophile trace elements are at concentrations unlike those of cumulate eucrites. There is also no textural evidence for cumulus processes. Although lithic clasts represent a variety of textural types, mineral compositions and bulk compositions of all of these materials are similar (Vaya et al., 1996; Buchanan et al., 1997a, b; Shukla et al., 1997a, b).

Hence, Piplia Kalan is probably most accurately classified as a genomict breccia, rather than as a monomict or polymict eucrite.

On a plot of Sc vs. La (Fig. 8), main group eucrites and Stannern form a horizontal array of nearly constant Sc with decreasing La content. In contrast, main group eucrites and Nuevo Laredo are distinguished by increasing Sc and La and apparently represent a continuous spectrum of compositions formed by increasing fractional crystallization of a primitive melt similar in composition to the main group eucrite Sioux County. Five of the seven Piplia Kalan analyses (this work; Shukla et al., 1997a) plot between main group eucrites and Vetluga, considered by Lindstrom and Mittlefehldt (1992) to be a Nuevo Laredo-trend eucrite. Piplia Kalan also has a FeO content intermediate between those of main group eucrites and Nuevo Laredo. Hence, because of its intermediate composition, Shukla et al. (1997a) classified Piplia Kalan as a Nuevo Laredo-trend eucrite. We believe that Piplia Kalan, like Vetluga, represents an intermediate composition on the fractional crystallization trend, and that the main group eucrites and Nuevo Laredo should be referred to as the Nuevo Laredo-trend.

Igneous Petrology. Bulk compositions of individual samples of lithic clasts and the brecciated matrix of the meteorite (Table 5 of this study; Shukla et al., 1997a) deserve additional comment. On the plot of Sc vs. La (Fig. 8), compositions of fine-grained lithology A and the matrix of Piplia Kalan form a cluster. In contrast, analyses of lithology B display a broader range of compositions, which extend to lower abundances of Sc and La, although one of the analyses reported by Shukla et al. (1997a) also falls close to the cluster of compositions of finer-grained samples. These compositional differences are plausibly due to heterogeneities caused by non-representative sampling of the coarser-grained lithology B. In comparison, the dashed field in Fig. 8 encloses the range of individual analyses, taken from the literature, of Juvinas, a

relatively coarse-grained eucrite. This compositional range is substantially larger than the field of Piplia Kalan analyses.

The wide range of textures of lithic clasts included within Piplia Kalan apparently results from differences in cooling rates. Hornfelsic materials originally were hypocrystalline or variolitic in texture; similar textures are not uncommon among terrestrial basalts and are characteristic of melts that quenched or crystallized very quickly. Similar hypocrystalline materials have been described from several eucrites including Pasamonte and Stannern (Basaltic Volcanism Study Project, 1981). In contrast, ophitic/subophitic materials cooled more slowly, with increasing grain size generally correlated with decreasing cooling rate. This variation in texture among lithic clasts that are similar in composition suggests derivation from the same lava flow or shallow intrusive body with hypocrystalline materials representing the fine-grained outer margin and coarser-grained ophitic/subophitic clasts representing the more slowly cooled interior.

Early brecciation. After crystallization of mafic liquids, Piplia Kalan was exposed to at least one early episode of brecciation, which formed lithic clasts and fine-grained matrix of the meteorite. Evidence that the lithologies contained within Piplia Kalan were subjected to shock includes undulating extinction of minerals, incipient mosaicism of feldspar, and deformed twins in feldspar (Vaya et al., 1996; Shukla et al., 1997a). Shock associated with this early episode of brecciation is also the most reasonable explanation for areas of lithology B that are composed of aggregates of granular pyroxene and opaque minerals between laths of deformed feldspar. We suggest these areas represent shocked ophitic/subophitic material that was later metamorphosed. Pyroxenes were granulated and later recrystallized; feldspars were deformed.

Piplia Kalan is distinct from most other equilibrated, noncumulate eucrites in that it contains a high proportion of lithic clasts as compared to matrix material. This fact and the close apparent petrogenetic relationship of all of the materials contained in the meteorite suggest that this early brecciation event may have been a low energy impact that caused limited shock, displacement, and brecciation effects. Alternatively, the environment sampled by this meteorite may have been characterized by small amounts of displacement below or on the periphery of a more energetic impact.

Metamorphism. Several features suggest that all of the materials in Piplia Kalan were subjected to extensive metamorphism. Most of the clasts in Piplia Kalan are metavolcanic rocks, which have, to a greater or lesser extent, been recrystallized to hornfelsic textures. Terrestrial volcanic rocks that were affected by increased temperature and low pressure typical of contact metamorphism display similar textures. Clouding of minerals similar to that displayed by lithologies A and B is found among metamorphosed Tertiary lavas sampled ~ 0.5 m from the contact with the Cuillin layered igneous complex on the Isle of Skye (Hutchison and Bevan, 1977). The centers of pyroxenes in these metabasalts commonly display abundant small inclusions along preferred crystallographic planes. Feldspars in these rocks also contain abundant inclusions. Almond (1964) described, within some of these metavolcanic rocks, feldspar phenocrysts with scalloped edges, which are similar to those in lithology C of Piplia Kalan and are the result of the recrystallization of adjacent pyroxenes. The report by Vaya et al. (1996) of xenoliths of lithology C within clasts of lithology A may indicate that metamorphism of some of these materials resulted when quickly-cooled materials from the outer margins of the flow or shallow intrusive body were broken up and entrained within the melt during flow.

Textural evidence suggests that at least part of the metamorphism experienced by Piplia Kalan was late-stage. The nonporous texture of the brecciated matrix suggests that the meteorite was exposed to an episode of thermal metamorphism after the original brecciation event. Hewins (1979) and Buchanan and Reid (1996) reported similar textures in the Petersburg polymict eucrite; Fe-rich diffusion boundaries around magnesian orthopyroxene fragments and redistribution of metal grains into 'spongy' textures accompany these features. Hewins (1979) and Buchanan and Reid (1996) interpreted these features as the result of post-aggregation thermal metamorphism. These textural data confirm the suggestion by Bhandari et al. (1998) that Piplia Kalan experienced thermal metamorphism late in its petrogenetic history, and the 2.2 Ga K-Ar age may date this thermal event.

Late shock event. Glassy veins that traverse both lithic clasts and brecciated matrix in Piplia Kalan are not recrystallized and thus were formed after thermal metamorphism. These veins apparently resulted from a late-stage shock event, which may have been the impact that ejected Piplia Kalan from its parent body. Similar shock-produced glass veins have been reported in the eucrites Cachari (Fredriksson and Kraut, 1967) and Stannern (Duke and Silver, 1967). However, the Cachari glass veins are 3.0 Ga old (Bogard et al., 1985) and, thus, are older than the impact that launched this meteorite from the eucrite parent body. The vein analyzed in this study is enriched in feldspar compared to the bulk composition of Piplia Kalan and compared to most eucrites; it apparently formed by shock melting of an area of the meteorite that was locally feldspar-enriched.

5. CONCLUSIONS

Piplia Kalan is distinctive compared to most other brecciated eucrites because of the high volumetric proportion of lithic clasts as compared to matrix, and because the various lithologies represented among these lithic clasts are similar in mineralogy and bulk composition, but differ in texture and grain size. These features suggest that the various lithologies represented in Piplia Kalan are samples of different parts of a single lava flow or shallow intrusive body. Nonporous matrix textures, the abundant inclusions contained within pyroxene and plagioclase grains, and the recrystallization evident in the hornfelsic lithic clasts suggest that these materials were subjected to one or more episodes of thermal metamorphism and that at least one of these episodes occurred after initial brecciation and aggregation of the meteorite. The presence of glass veins traversing matrix and lithic clasts indicates that after thermal metamorphism, Piplia Kalan experienced an episode of shock, which may have resulted in ejection of the meteorite from the HED parent body.

Acknowledgments- We are indebted to Penny Bernhard at NASA-JSC and to the Council of Geosciences of South Africa for producing excellent thin sections of Piplia Kalan. Vincent Yang and Franz Brandstätter provided technical assistance with electron microprobe analysis. Discussions with Arch Reid, Don Bogard, Larry Nyquist, and Bevan French are greatly appreciated. This work was supported by the Austrian Fonds zur Förderung der wissenschaftlichen Forschung, START-Y58. Also providing funds were NASA RTOP #344-31-10-17 to D.J. Lindstrom and NASA RTOP #152-13-40-21 to M.M. Lindstrom.

REFERENCES

Almond D.C. (1964) Metamorphism of Tertiary lavas in Strathaird, Skye. *Trans. Roy. Soc. Edin.* **65**. 413-434.

Anders E. and Grevesse N. (1989) Abundances of the elements: Meteoritic and solar. *Geochim. Cosmochim. Acta* **53**, 197-214.

Basaltic Volcanism Study Project (1981) *Basaltic Volcanism on the Terrestrial Planets.* Pergamon. 1286 p.

Bhandari N., Murthy S.V.S., Suthar K.M., Shukla A.D., Ballabh G.M., Sisodia M.S., and Vaya V.K. (1998) The orbit and exposure history of the Piplia Kalan eucrite. *Meteorit. Planet. Sci.* **33**, 455-461.

Bogard D.D., Taylor G.J., Keil K., Smith M.R., and Schmitt R.A. (1985) Impact melting of the Cachari eucrite 3.0 Gy ago. *Geochim. Cosmochim. Acta* **49**, 941-946.

Buchanan P.C. and Reid A.M. (1996) Petrology of the polymict eucrite Petersburg. *Geochim. Cosmochim. Acta* **60**, 135-146.

Buchanan P.C., Coetzee S.H., Reimold W.U., and Reid A.M. (1997a) Petrography and mineral chemistry of the Pipliya eucrite (abstract). *Lunar Planet. Sci.* **28**, 167-168.

Buchanan P.C., Mittlefehldt D.W., Hutchison R., Pandit M.K., and Koeberl C. (1997b) Petrogenetic history of the Piplia Kalan eucrite (abstract). *Meteorit. Planet. Sci.* **32**, supp., A22-A23.

Christophe Michel-Levy M., Bourot-Denise M., Palme H., Spettel B., and Wanke H. (1987) L'eucrite de Bouvante: chimie, petrologie et mineralogie. *Bull. Mineral.* **110**, 449-458.

Duke M.B. and Silver L.T. (1967) Petrology of eucrites, howardites, and mesosiderites. *Geochim. Cosmochim. Acta* **31**, 1637-1665.

von Engelhardt W. (1963) Die eukrit von Stannern. *Bei. Min. Petr.* **9**, 65-94.

Fredriksson K. and Kraut F. (1967) Impact glass in the Cachari eucrite. *Geochim. Cosmochim. Acta* **31**. 1701-1704.

Harlow G.E. and Klimentidis R. (1980) Clouding of pyroxene and plagioclase in eucrites: implications for post-crystallization processing. *Proc. Lunar Planet. Sci. Conf.* **11**, 1131-1148.

Harlow G.E., Nehru C.E., Prinz M., Taylor G.J., and Keil K. (1979) Pyroxenes in Serra de Magé: cooling history in comparison with Moama and Moore County. *Earth Planet. Sci. Ltrs.* **43**. 173-181.

Hewins R.H. (1979) The composition and origin of metal in howardites. *Geochim. Cosmochim. Acta* **43**. 1663-1673.

Hutchison R. and Bevan J.C. (1977) The Cuillin layered igneous complex-evidence for multiple intrusion and former presence of a picritic liquid. *Scott. J. Geol.* **13**, 197-210.

Jérome D.Y. (1970) *Composition and origin of some achondritic meteorites*. Ph.D. dissertation, Univ. of Oregon. 166 p.

Kvasha L.G. and Dyakonova M.I. (1972) The Pomozdino eucrite. *Meteoritika* **31**, 109-115.

Lindstrom M.M. and Mittlefehldt D.W. (1992) A geochemical study of Russian eucrites and howardites (abstract). *Meteoritics* **27**, 250.

Mittlefehldt D.W. (1979) Petrographic and chemical characterization of igneous lithic clasts from mesosiderites and howardites and comparison with eucrites and diogenites. *Geochim. Cosmochim. Acta* **43**, 1917-1935.

Mittlefehldt D.W. and Lindstrom M.M. (1991) Generation of abnormal trace element abundances in Antarctic eucrites by weathering processes. *Geochim Cosmochim. Acta* **55**, 77-87.

Mittlefehldt D.W., See T.H., and Horz F. (1992) Dissemination and fractionation of projectile materials in the impact melts from Wabar Crater, Saudi Arabia. *Meteoritics* **27**, 361-370.

Palme H., Baddenhausen H., Blum K., Cendales M., Dreibus G., Hofmeister H., Kruse H., Palme C., Spettel B., Vilcsek E., and Wänke H. (1978) New data on lunar samples and achondrites and a comparison of the least fractionated samples from the earth, the moon, and the eucrite parent body. *Proc. 9th Lunar Planet. Sci. Conf.*, 25-57.

Reid A.M. and Barnard B.M. (1980) Unequilibrated and equilibrated eucrites (abstract). *Lunar Planet. Sci.* **11**. 1019-1021.

Schmitt R.A., Smith R.H., Lasch J.E., Mosen A.W., Olehy D.A., and Vasilevskis R.G. (1963) Abundances of the fourteen rare-earths, scandium, and yttrium in meteoritic and terrestrial matter. *Geochim. Cosmochim. Acta.* **29**, 498-512.

Schmitt R.A., Smith R.H., and Olehy D.A. (1964) Rare-earth, yttrium and scandium abundances in meteoritic and terrestrial matter-II. *Geochim. Cosmochim. Acta.* **28**, 67-86.

Shukla A.D., Shukla P.N., Suthar K.M., Bhandari N., Vaya V.K., Sisodia M.S., Sinha Roy S., Rao K.N., and Rajawat R.S. (1997a) Piplia Kalan eucrite: Fall, petrography, and chemical characteristics. *Meteorit. Planet. Sci.* **32**, 611-615.

Shukla A.D., Bhandari N., Shukla P.N., Natarajan R., and Sisodia M.S. (1997b) Chemistry and petrography of the Piplia Kalan eucrite (abstract). *Meteorit. Planet. Sci.* **32**, supplement, A120.

Srinivasan G., Goswami J.N., and Bhandari N. (1999) ^{26}Al in eucrite Piplia Kalan: plausible heat source and formation chronology. *Science* **284**, 1348-1350.

Takeda H. and Graham A.L. (1991) Degree of equilibration of eucritic pyroxenes and thermal metamorphism of the earliest planetary crust. *Meteoritics* **26**, 129-134.

Vaya V.K., Mehta D.S., Bafna P.C., Sisodia M.S., and Shrivastava K.L. (1996) The Pipliya meteor shower: A preliminary study. *Current Science* **71**, 253-257.

Wänke H., Baddenhausen H., Blum K., Cendales M., Dreibus G., Hofmeister H., Kruse H., Jagoutz E., Palme C., Spettel B., Thacker R., and Vilcsek E. (1977) On the chemistry of lunar samples and achondrites. Primary matter in the lunar highlands: a reevaluation. *Proc. 8th Lunar Sci. Conf.*, 2191-2213.

Warren P.H. and Jerde E.A. (1987) Composition and origin of Nuevo Laredo trend eucrites. *Geochim. Cosmochim. Acta* **51**, 713-725.

Warren P.H., Jerde E.A., Migdisova L.F., and Yaroshevsky A.A. (1990) Pomozdino: an anomalous, high-MgO/FeO, yet REE-rich eucrite. *Proc. 20th Lunar Planet. Sci. Conf.*, 281-297.

Zavaritskii A.N. and Kvasha L.G. (1952) *Meteorites of the U.S.S.R.* Academy of Sciences of the U.S.S.R.

Table 1. Composition of glass (in wt. %) from a vein in Piplia Kalan acquired by electron microprobe analysis (ave. of 5 analyses).

SiO_2	48.0
TiO_2	0.39
Al_2O_3	21.4
Cr_2O_3	0.08
FeO	11.2
MnO	0.35
MgO	3.63
CaO	13.2
NiO	0.01
Na_2O	0.76
K_2O	0.05
Total	99.1

Table 2. Representative compositions (in wt. %) determined by electron microprobe of pyroxenes in matrix and various lithologies of Piplia Kalan.

	Matrix		Lithology A		Lithology B		Hornfelsic Clasts	
SiO_2	50.7	48.9	50.4	49.4	51.0	49.6	51.6	50.3
TiO_2	0.25	0.16	0.34	0.19	0.26	0.15	0.18	0.11
Al_2O_3	0.46	0.13	0.62	0.20	0.37	0.14	0.25	0.08
Cr_2O_3	0.23	0.04	0.18	0.11	0.17	0.09	0.14	0.03
FeO	16.7	36.8	16.2	35.0	16.6	36.1	16.6	37.5
MnO	0.45	1.12	0.47	1.13	0.49	1.1	0.48	1.22
MgO	9.6	11.4	9.63	11.2	9.85	11.6	10.1	11.5
CaO	20.6	1.05	21.2	2.63	21.0	1.02	20.9	0.99
Total	99.0	99.6	99.0	99.9	99.7	99.8	100.3	101.7
Wo	43.8	2.3	44.9	5.8	44.1	2.2	43.6	2.1
En	28.4	34.8	28.3	34.2	28.7	35.6	29.3	34.6
Fs	27.8	62.9	26.8	60.0	27.2	62.2	27.1	63.3

Table 3. Representative compositions (in wt. %) determined by electron microprobe of feldspars in matrix and various lithologies of Piplia Kalan.

	Matrix		Lithology A		Lithology B		Hornfelsic Clasts	
SiO_2	46.2	44.6	45.7	44.8	44.8	45.1	45.5	46.4
TiO_2	0.02	b.d.	0.02	0.01	b.d.	b.d.	b.d.	0.02
Al_2O_3	35.4	35.4	35.4	35.6	34.9	35.3	35.9	34.9
FeO	0.18	0.35	0.49	0.29	0.18	0.75	0.38	0.70
MgO	b.d.	b.d.	b.d.	b.d.	b.d.	b.d.	0.02	0.01
CaO	17.1	18.2	17.9	17.4	18.1	18.1	18.2	18.3
Na_2O	1.35	1.11	1.29	1.35	1.34	1.16	1.16	1.14
K_2O	0.09	0.08	0.07	0.08	0.08	0.08	0.04	0.03
Total	100.3	99.7	100.9	99.5	99.4	100.5	101.2	101.5
Or	0.5	0.5	0.4	0.5	0.5	0.5	0.2	0.2
Ab	12.5	9.9	11.5	12.2	11.8	10.3	10.3	10.1
An	87.0	89.6	88.1	87.3	87.8	89.2	89.5	89.7

b.d.<0.01

Table 4. Representative compositions (in wt. %) determined by electron microprobe of minor minerals in matrix and various lithologies of Piplia Kalan.

	Matrix		Lithology A			Lithology B	Hornfelsic Clast
	ilm.	ilm.	ilm.	ilm.	cr. sp.	ilm.	ilm.
TiO_2	52.6	52.1	52.7	51.4	3.17	52.1	53.4
Al_2O_3	b.d.	0.02	b.d.	0.10	10.3	b.d.	0.03
Cr_2O_3	0.06	0.39	0.14	1.80	50.5	0.38	0.36
FeO	44.3	44.2	44.8	44.4	35.0	45.0	45.7
MnO	0.86	0.87	0.95	0.86	b.d.	0.94	0.80
MgO	0.66	0.51	0.43	0.39	0.27	0.49	0.58
CaO	0.14	0.32	0.03	0.12	0.05	0.09	0.38
NiO	b.d.	b.d.	0.01	b.d.	b.d.	b.d.	b.d.
Total	98.6	98.4	99.1	99.1	99.3	99.0	101.3

b.d.<0.01

Table 5. Compositions determined by INAA of lithologies A and B and of the matrix of Piplia Kalan (this work) compared with mean of literature data for Juvinas*.

		lithology A finer-grained	lithology B coarser-grained	matrix	Juvinas literature mean*
mass (mg)		88.61	84.41	65.35	
Na_2O	(wt%)	0.477	0.497	0.462	0.431
K	(ppm)	320	260	320	340
CaO	(wt%)	10.1	9.9	9.9	10.7
Sc	(ppm)	32.0	28.6	32.3	28.9
Cr_2O_3	(wt%)	0.343	0.379	0.303	0.286
FeO	(wt%)	19.2	18.9	19.2	18.0
Co	(ppm)	5.25	4.03	4.65	4.61
La	(ppm)	2.73	2.60	3.11	2.59
Ce	(ppm)	7.8	7.0	8.0	6.8
Sm	(ppm)	1.78	1.60	1.94	1.62
Eu	(ppm)	0.62	0.64	0.62	0.62
Tb	(ppm)	0.44	0.42	0.48	0.42
Yb	(ppm)	1.84	1.68	1.92	1.68
Lu	(ppm)	0.265	0.248	0.281	0.248
Hf	(ppm)	1.41	1.27	1.52	1.19
Ta	(ppb)	200	140	180	160
Th	(ppb)	290	270	320	290

* The Juvinas literature mean is taken from a comprehensive database of HED analyses maintained by DWM.

Figure Captions

Fig. 1. Photomicrograph in transmitted light of part of a shocked eucritic clast with ophitic/subophitic texture. Feldspar laths are continuous, whereas pyroxene varies from a large continuous crystal at the left of the photo to a fine-grained granular texture in the center of the photo. Long axis of the photo is 1 mm.

Fig. 2. a) Photomicrograph in transmitted light of lithology C (left side of photo). Long axis of photo is ~2 mm. b) Photomicrograph in transmitted light of a partially recrystallized lath-shaped pyroxene in lithology C. Long axis of photo is 1 mm.

Fig. 3. Back-scattered electron image (BSEI) of the brecciated matrix of Piplia Kalan. Note the lack of porosity.

Fig. 4. BSEI of a glass vein (medium grey; arrow) in Piplia Kalan. Long axis of the image is ~0.1 mm.

Fig. 5. Photomicrograph in transmitted light of 'clouding' (arrows) of pyroxene and feldspar in lithology B. Long axis of the photo is 2.5 mm.

Fig. 6. Compositions of pyroxenes in Piplia Kalan lithologies. The fields outlined in the diagram for matrix pyroxenes are those of pyroxenes in Juvinas (J) and Nuevo Laredo (NL) (Basaltic Volcanism Study Project, 1981).

Fig. 7. Rare-earth-element diagram of Piplia Kalan lithologies compared to other noncumulate eucrites. The REE patterns for Juvinas, Nuevo Laredo, Sioux County, and Stannern are based on averaged abundances computed from data published in the literature and unpublished JSC data. Data sources include Basaltic Volcanism Study Project (1981), Christophe Michel-Levy et al. (1987), von Engelhardt (1963), Jérome (1970), Kvasha and Dyakonova (1972), Mittlefehldt

(1979), Palme et al. (1978), Schmitt et al. (1963, 1964), Wänke et al. (1977), and Warren and Jerde (1987). Abundances are normalized to Anders and Grevesse (1989).

Fig. 8. A La vs. Sc diagram comparing individual analyses of Piplia Kalan (this work, Shukla et al., 1997a) to averages for other noncumulate eucrites computed from data published in the literature and unpublished JSC data. Arrows indicate the Stannern-trend (St) and the Nuevo Laredo-trend (Nt). Symbols: lithology A (fg, grey circles), lithology B (cg, dark filled circles), Piplia Kalan matrix (m, small filled square), 'main group' eucrites (open circles), Nuevo Laredo-trend eucrites (stars), Stannern-trend (filled diamonds). The dashed field is the range of bulk compositions for analyzed samples of Juvinas. Labeled eucrites are Vetluga (V) (Lindstrom and Mittlefehldt, 1992), Lakangaon (L), and Nuevo Laredo (N). Anomalous eucrites (open diamonds) are ALHA81001 (A) (Warren and Jerde, 1987) and Pomozdino (P) (Warren et al., 1990). Data sources include Basaltic Volcanism Study Project (1981), Christophe Michel-Levy (1987), von Engelhardt (1963), Jérome (1970), Kvasha and Dyakonova (1972), Mittlefehldt (1979), Palme et al. (1978), Schmitt et al. (1963, 1964), Wänke et al. (1977), Warren and Jerde (1987), Zavaritskii and Kvasha (1952), and unpublished JSC data.

Fig. 1

A

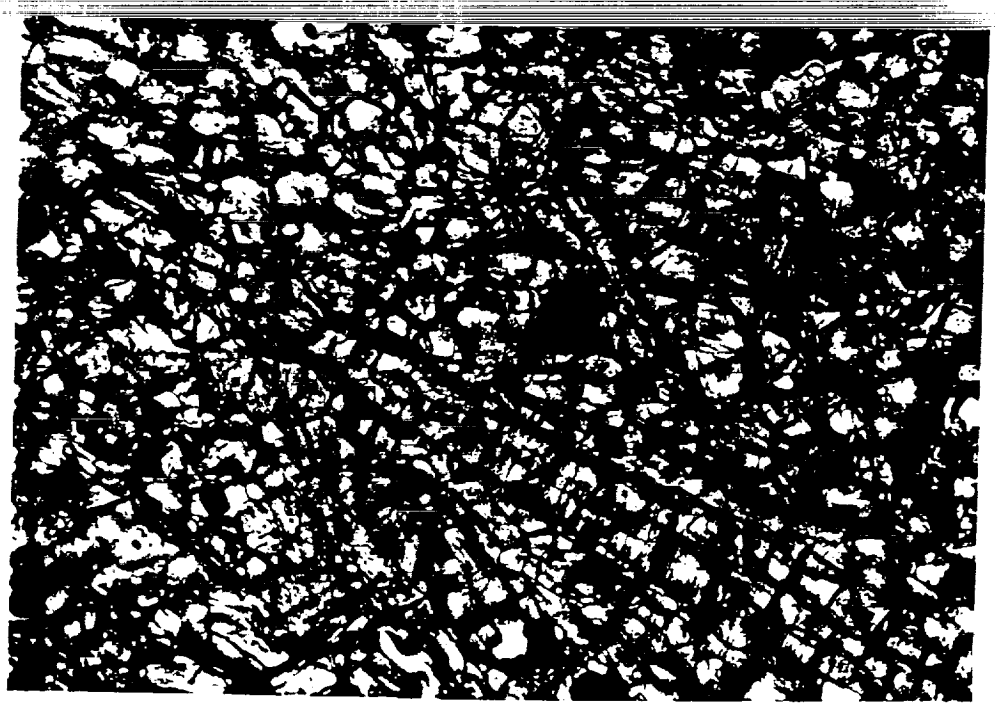

B

Fig. 2

Fig. 3

Fig. 4

Fig. 5

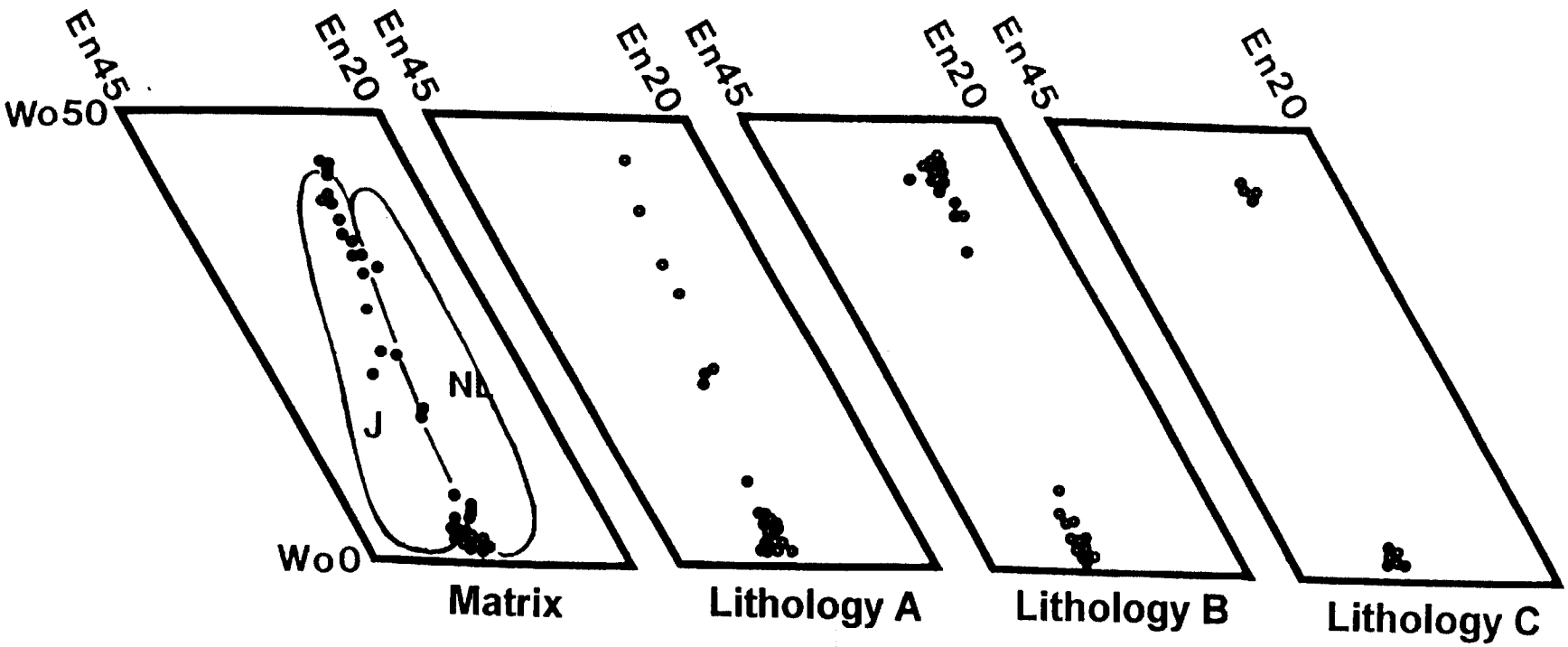
En45
En20
En45
En20
En45
En20
En45
En20
Wo50
Wo0
J
NL
Matrix
Lithology A
Lithology B
Lithology C

Fig. 6

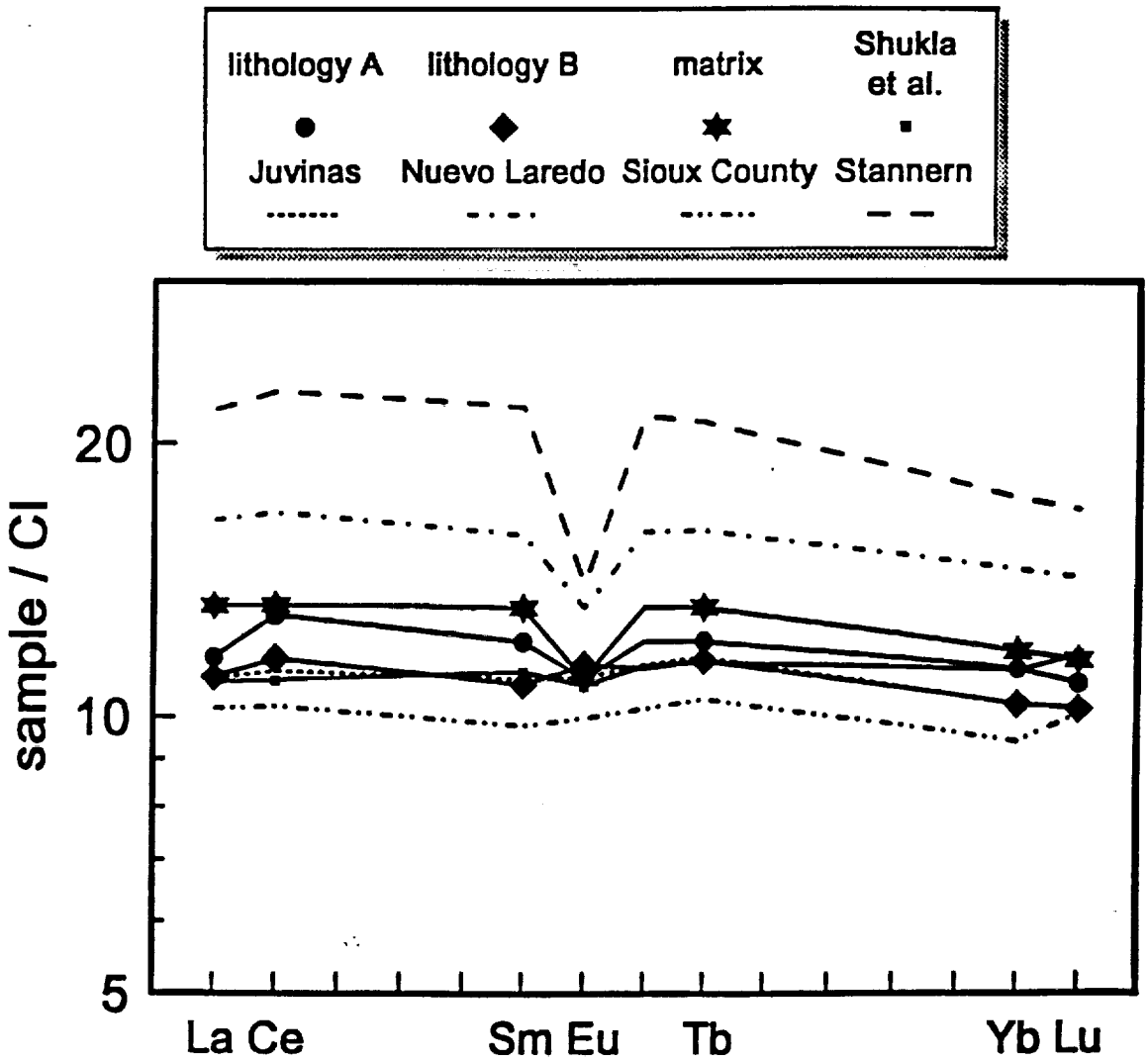
lithology A
lithology B
matrix
Shukla et al.
Juvinas
Nuevo Laredo
Sioux County
Stannern
sample / CI
20
10
5
La Ce
Sm Eu
Tb
Yb Lu

Fig. 7

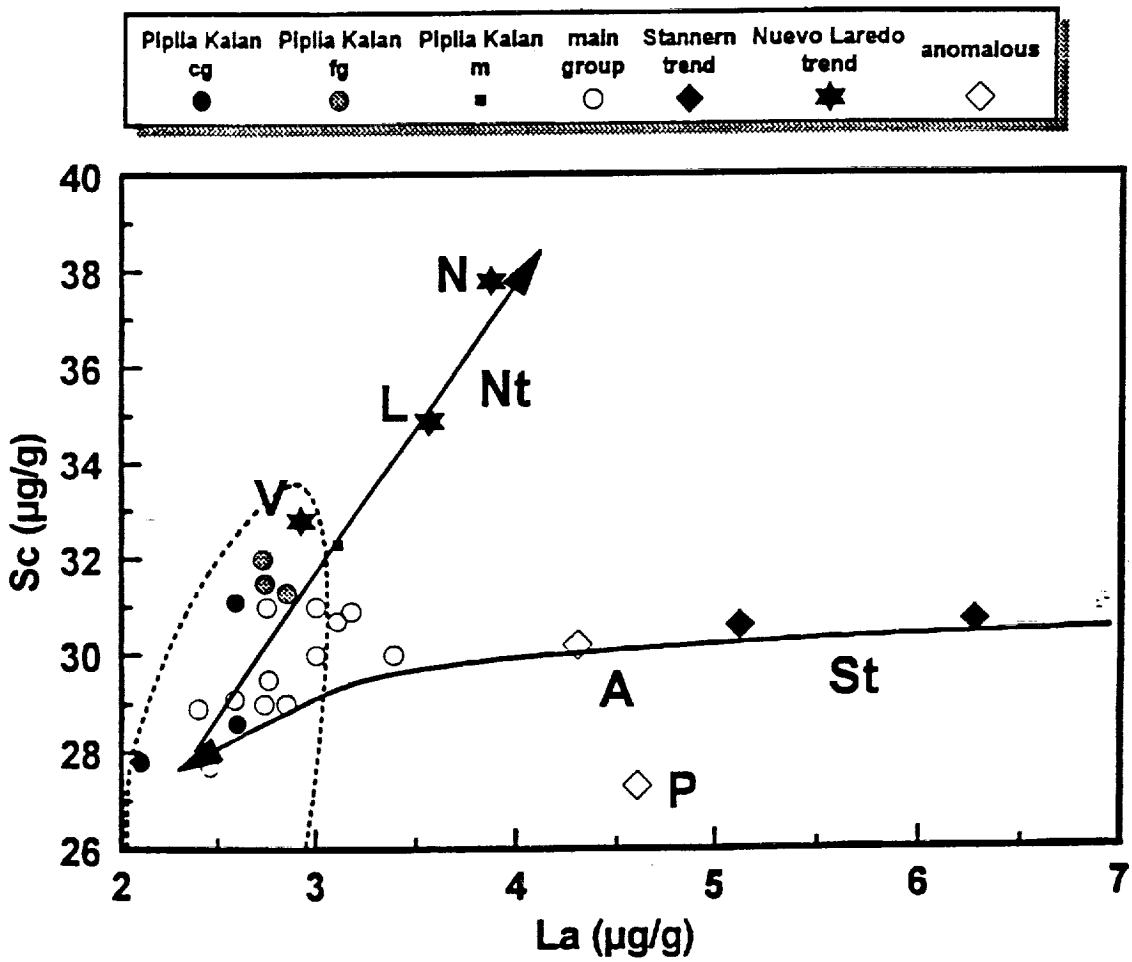
Piplia Kalan cg
Piplia Kalan fg
Piplia Kalan m
main group
Stannern trend
Nuevo Laredo trend
anomalous
Sc (µg/g)
La (µg/g)
N
Nt
L
V
A
St
P
40
38
36
34
32
30
28
26
2
3
4
5
6
7

Fig. 8